ORIGINAL PAPER

Improvement of Endothelial Cell Performance in an Optimized Electrospun Pre-polyglycerol Sebacate-Poly Lactic Acid Scaffold for Reconstruction of Intima in Coronary Arteries

Soodabeh Gorgani[1] · Anousheh Zargar Kharazi[1,2] · Shaghayegh Haghjooy Javanmard[2] · Mohammad Rafiinia[3]

Abstract

A most important parameter in tissue engineering of blood vessels is the restoration of the endothelium in small-diameter vascular grafts. Not only the mechanical properties of the inner layer of the synthetic graft but also its physical and chemical properties play important roles in both the response of the endothelial cells and the successful reconstruction of the lumen layer. This study was conducted to develop an optimized scaffold of pre-polyglycerol sebacate-poly lactic acid (pre-PGS-PLLA) polymeric blend and to determine the relevant electrospinning parameters that guarantee the required tensile strength, failure strain, and Young's modulus of the graft. A second aspect of the study involved evaluation of the suture strength, burst strength, water contact angle, degradation rate, and the response of Human Umbilical Vein Endothelial Cells to the fabricated scaffold. The pre-PGS-PLLA blend showed a tensile strength of 0.420 ± 0.23 MPa, a Young's modulus of 2.05 ± 0.27 MPa, a suture strength with a failure strain of $67.6 \pm 10.97\%$, and a burst strength of 90.2 ± 0.95 kPa, all of which were mechanically consistent with the artery intima characteristics. Moreover, a contact angle of $> 10°$ with water was recorded. The scaffold was found capable of maintaining 40.14% of its initial weight after 60 days while also retaining its structural integrity. Based on the HUVEC cell response examination, the scaffold had no toxicity and the cells showed satisfactory morphology and proliferation. Given the proper imitation of the mechanical properties as well as the survival and proliferation of the endothelial cells, the synthesized scaffold may be recommended for the reconstruction of coronary artery intima and the treatment of vascular tissue disorders.

Keywords Tissue engineering of vascular grafts · Intima reconstruction · Pre-poly polyglycerol sebacate · Poly lactic acid · Electrospinning

Introduction

Endothelium and intima malfunctioning is characteristic of cardiovascular and cerebrovascular diseases. Despite the numerous solutions so far proposed by scientists and vascular surgeons, small-diameter vessel reconstruction still remains a challenge awaiting resolution. In such diseases endothelium needs restoration in order to reduce the progression of vascular diseases in humans [1, 2]. Scaffolds with the same functions of blood vessels fabricated through tissue engineering of blood vessels (TEBV) should enjoy mechanical properties consistent and compatible with the physiological properties of vessels since cell behavior is not only affected by the chemical properties of the surrounding media, but also influenced by the physical and mechanical properties of the surface on which the cell is attached [3].

Interactions between cells and their mechanical environment give rise to cellular responses that play important roles in controlling cell behavior. Among the mechanical stimuli, the substrate elastic modulus is known as a determinant of cellular behavior through mechano-transduction pathways. Experimental studies have shown the effects of substrate

✉ Anousheh Zargar Kharazi
a_zargar@med.mui.ac.ir; anosh_zargar@yahoo.com

1   Department of Biomaterials, Nanotechnology and Tissue Engineering, School of Advanced Technologies in Medicine, Isfahan University of Medical Sciences, Isfahan, Iran

2   Applied Physiology Research Center, Cardiovascular Research Institue, Isfahan University of Medical Sciences, Isfahan, Iran

3   Department of Biomaterials and Tissue Engineering, Biosensor Research Center, Isfahan University of Medical Sciences, Isfahan, Iran

elastic modulus on such varied types of cells as myocytes, fibroblasts, epithelial cells, cancer cells, and stem cells. Regarding the importance of recognizing the behavior of endothelial cells towards substrates of different elastic moduli, studies have been conducted to investigate the effects of substrate stiffness on endothelium behavior, such as cell morphology, proliferation, adhesion, migration, arteriogenesis, and survival rate [3–5].

Scaffolds similar in mechanical properties to the living tissue improve cell life and connection through enrichment of lamellipodia and filopodia among the endothelial cells, thereby affecting cellular behavior. As the main mechanical property of the cell substrate, elasticity modulus can be used for the in vitro simulation of the mechanical conditions of tissues [6, 7].

Electrospinning is a suitable technique for synthesizing vascular scaffolds. In this method, fibers of different diameters can be produced by changing the electrospinning parameters to achieve the desired structural and mechanical properties in the scaffold. In addition, good cell attachment and proliferation can be ensured by creating ECM-like morphologies. A wide number of studies have, therefore, used electrospun biodegradable polymers to produce vascular scaffolds with the desired properties [8]. None has, however, proved capable of specifically optimizing the human intima. For example, Carrabba and Madeddu used an acellular electrospun PCL tubular scaffold in the carotid artery of rats to observe that endothelium and neo-intima layers formed within 28 days in the anastomosis regions [9]. Putzu et al. cultured HUVEC cells on an electrospun SILK-ELP biopolymer scaffold used for the reconstruction of intima and placed it in rabbit aorta to observe the formation of neo-intima [10]. Javanmard and Anari synthesized a three-layered vascular graft by sequential electrospinning of PCL, collagen, and PLLA nanofibers on which HUVEC endothelial cells were cultured. The authors found that not only were the mechanical properties of this scaffold similar to those of the saphenous vein but also that the scaffold exhibited good metabolic and cytocompatibility activities [11]. It seems that the resulting mechanical properties do not imitate those of LAD artery intima. Moreover, the formation of neo-intima has been mentioned as an indicator of the proliferation of vessels' smooth muscle cells (SMCs), which proliferate and form the neo-intima in competition with endothelial cells that have experienced prolonged degradation [12, 13].

PLLA, often used as a copolymer in tissue engineering scaffolds due to its low degradation rate [15, 16], is a synthetic polymer with proper biocompatibility, hemocompatibility [14], and mechanical properties. Another polymer also used in diverse biomedical applications is PGS that is a biocompatible, hemocompatible, biodegradable elastomer. In vitro and in vivo studies have revealed its good biocompatibility with the least inflammation and fibrotic response

of PGS implants. Surface degradation of PGS occurs with a linear profile in vivo and is completely absorbed in a month. Another advantage of PGS scaffolds is that their mechanical properties can be controlled by the cross-link process and optimized according to the specific requirements of the tissue [17–19]. While both PLLA and PGS have been approved by the Food and Drug Administration (FDA), it seems desirable to manufacture scaffolds by combining these polymers in a proper ratio to achieve mechanical properties and degradation rates appropriate for vascular tissue engineering. The present study is thus devoted to optimizing the pre-PGS-PLLA blend and the electrospinning parameters in order to synthesize such scaffolds with proper mechanical properties.

Materials and Methods

Materials

PLLA (RESOMER L210S) and Glycerol (G5516) were purchased from Sigma Aldrich. Sebacic acid (S18609053 581), chloroform (K46962445), and acetone (K45354714) were obtained from Merck. Prolene suture was purchased from Shahid Rajaee Heart Hospital of Tehran.

Scaffold Synthesis

Glycerol and sebacic acid were used as monomers to produce pre-PGS via condensation polymerization at a high temperature. Briefly, sebacic acid and glycerol were mixed at a molar ratio of 1:1 under the nitrogen atmosphere at 130 °C in an oil bath for 6 h to obtain a white PGS pre-polymer. The functional groups of the polymer were studied by Fourier transform infrared (FTIR) spectroscopy to evaluate the polymer structure. Subsequently, pre-PGS:PLLA solutions were prepared at weight ratios of 1:1, 2:1, and 3:1 using acetone:dimethylformamide (1:1 v/v) and pre-PGS:PLLA scaffolds were fabricated using the electrospinning method. Electrospinning parameters were varied as reported in Table 1 to achieve uniform fibers without any beads.

Characterization of the Scaffold Structure

The surface porosity, fiber diameter, and morphology of the synthesized scaffolds were evaluated by scanning electron microscopy (SEM). The surface porosity of the scaffolds and their interconnectivity were estimated using MATLAB version 2015 [20]. The functional groups of the chemical bonds of the pre- PGS:PLLA scaffold were evaluated by Fourier transform infrared spectroscopy (FTIR, AVATAR model, Thermo).

Table 1 Electrospinning parameters for different pre-PGS-PLLA ratios

Ratio	Sample	Electrospinning conditions			
		Concentration (%)	Voltage (kV)	Distance (cm)	Feed rate (mL/h)
1:1	A1	35	15	25	40
	A2	12	20	30	40
2:1	B1	9	15	30	20
	B2	8	20	30	20
3:1	C1	12	15	30	10
	C2	12	20	18	10

Determination of Mechanical Properties

Tensile properties of the scaffolds were evaluated according to the ASTM D882 standard using Instron 5566 (USA). All the tensile tests were conducted at room temperature in a dry environment [21]. For this purpose, three specimens 1×1.5 cm in size were tested at a loading rate of 10 mm/min in ambient temperature and humidity to determine the tensile strength, elastic modulus, failure strain [21] while the burst strength of the specimens was measured using a bursting equipment (Burst brick, Brk109). Suture strength was measured using the Instron 5566 (USA) 2203 single-column benchtob universal tensile tester. For this purpose, the sutures were pulled at a rate of 50 mm/min until the grafts were completely torn apart.

Evaluation of the Degradation Rate

To assess the degradation rate for each time period (1, 7, 14, 21, 28, and 60 days), three samples were weighed using a GT2100 scale (USA) with an accuracy of ± 0.00001 and placed in a PBS solution. To evaluate weight loss over the specified durations, the samples were removed from the solution, dried at 37 °C in a vacuum oven for 60 min, and weighed. The results were plotted as percentage weight loss in each time point using Eq. (1) below:

$$W = (W_0 - W_t)/W_0 \times 100 \tag{1}$$

where, W_0 and W_t represent initial weight and the weight at the specified time, respectively. The results were reported as mean $\pm$ SD.

Contact Angle Measurement

To assess the hydrophobicity of the pre-PGS-PLLA scaffolds, the contact angle of the polymeric surface with a 7 μL water drop was measured at 25 °C (Jikan CAG-10). The recorded angles were then analyzed using image J: Drop Analysis software.

Cell Behavior

Cell Toxicity, Attachment, and Morphology

The toxicity of the samples and their effect on cell growth and proliferation were determined using the direct contact method. Briefly, 1×1.5 sheets were initially sterilized with 25 kGy gamma radiation at 25 °C before HUVEC cells (NCBI C554), obtained from the Cell Bank of Iran Pasteur Institute, were transferred after thawing to a flask containing Ham's F12 + DMEM medium with 10% FBS. The flask was then placed in an incubator at 37 °C, 90% humidity, and 5% oxygen. The culture medium was replaced every 3–4 days.

Diphenyl tetrazolium bromide (MTT, Sigma, USA) is one of the best indirect reagents to determine cell proliferation based on the change of the tetrazolium yellow powder to the dark purple insoluble crystalline of formazan. This phenomenon takes place only in living cells by the mitochondrial enzyme succinate dehydrogenase. Formazan crystals are dissolved by an organic solvent such as isopropanol and the resulting optical density (OD) is read. The recorded OD is proportional to the concentration of formazan, which is itself proportional to the metabolic activity of living cells. To evaluate cell proliferation, 1×10^4 cells in a 100 μL of the culture medium were applied on each of the sterile samples in the wells of a 24-well culture plate and then incubated at 37 °C for 4 h so that the cells would attach to the sample surface. Once cell attachment was ensured, 500 μL of the culture medium was added to each well. The supernatant over the cells was removed as much as possible after 1, 3, and 5 days before 300 μL of 0.5 mg/mL MTT was poured in each well. After 4 h of incubation, the supernatant over the cells was removed and 300 μL of isopropanol was added to dissolve the purple crystals produced. To improve the dissolution of the MTT sediment, the plate was placed on a shaker for 15 min. Then, 100 μL of the purple solution was transferred to the wells of a 96-well plate and the concentration of the compound dissolved in isopropanol was calculated using an ELISA reader (STAT FAX 2100, USA) at 570 nm. Wells with more cells in them exhibit higher OD values than those containing fewer cells. Hence, Eq. 2 below was used to identify wells with more cells for comparison with the control sample.

$$\text{Viability \%} = (\text{mean OD of sample})/(\text{mean OD of control}) \times 100 \tag{2}$$

To evaluate cell attachment, the sterile samples were placed in a 24-well plate. Then, 20,000 cells, 100 μL in volume, were poured on each sample and incubated for 4–5 h. After

cell attachment was investigated by SEM (AIS2300C), a certain amount of the culture medium containing 10% FBS was added to each well. The supernatant was removed after 1–2 days before the samples were washed with PBS for 30 s and 3.5% glutaraldehyde was added to each for cell fixation. The samples were then placed in a refrigerator for 2 h before the fixator was removed and the samples were washed with deionized water and then with 40, 60, 80, and 100% alcohol. Cell proliferation was evaluated at intervals of 1, 3, and 5 days.

Results and Discussion

Characterization of the Synthesized Pre-PGS Structure

Figure 1a depicts the FTIR spectrum of the synthesized pre-PGS. The stretch mode of the O–H bond produces a characteristic peak at 3400 cm^{-1} and peaks at 2921 and at mode [19, 20]. The peak at 2851 cm^{-1} can be attributed to alkene groups while absorption at 1696 cm^{-1} is assigned to the C=O stretch.
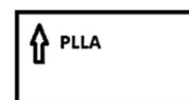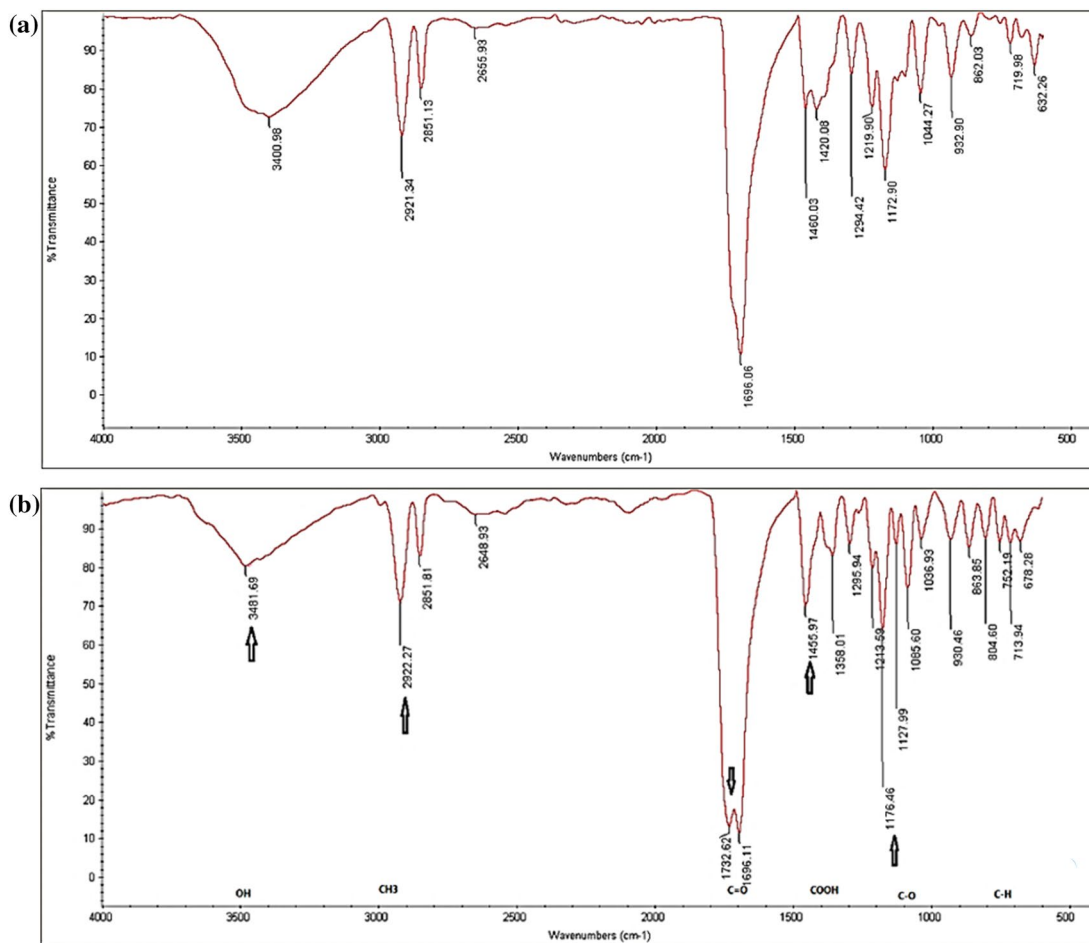
Fig. 1 FTIR spectrum of **a** the synthesized pre-PGS and **b** pre-PGS-PLLA blend (3:1)

Characterization of the Synthesized Pre-PGS-PLLA Blend

Figure 1b shows the FTIR spectrum of the pre-PGS-PLLA blend indicating characteristic peaks of the functional groups in pre-PGS and PLLA. The peak at 1036 cm^{-1} represents the stretch of C–O of the PLLA ester group, while that at 1355–1458 cm^{-1} is related to the asymmetric bending of the –CH$_2$– group. It should be mentioned that while C–O functional groups provide the possibility for hydrogen to bond with water molecules, the –CH$_2$– group modifies to a great extent the water absorption properties of the scaffold. Hence, the presence of the characteristic peaks of C–O and O–H groups confirms hydrogen bonding between these functional groups [22, 23].

Optimization of Electrospinning Parameters

Fiber morphology in three samples (A, B, and C) of the pre-PGS-PLLA blend solution was evaluated by SEM according to the variations produced in the electrospinning parameters reported in Table 2. Clearly, the fibers obtained from sample A are not appropriate due to their large diameters and lack of uniformity that fail them with respect to the required mechanical properties.

As already mentioned, it was the purpose of this study to restore the mechanical properties of the intima. It is obvious that fiber diameter and uniformity as well as polymer ratios play critical roles in the mechanical behavior of the final product. This is evidenced by the suitable solution viscosity

Table 2 Morphology of fibers obtained at different ratios of the pre-PGS_PLLA solution

Sample	Mean ± SD of fibers diameter (nm)	Porosity (%)	Descriptions
A1	2751 ± 948	85.18 ± 4.90	*High fiber diameter *Fiber non-uniformity *Low surface porosity rate
A2	2720 ± 101	62.15 ± 4.04	*High fiber diameter *Fiber non-uniformity *Low surface porosity rate
B1	2080 ± 790	50.91 ± 0.25	*Fiber uniformity *Proper fiber diameter *Low surface porosity rate
B2	1960 ± 780	98.82 ± 3.68	*High bead fibers
C1	950 ± 390	98.93 ± 2.21	*Proper fiber diameter *Proper surface porosity *Fiber uniformity
C2	1380 ± 270	80.38 ± 5.96	*Proper fiber diameter *Proper surface porosity rate

achieved with an increase in pre-PGS concentration in sample B while beaded fibers were formed at pre-PGS concentrations below 9% (Fig. 2). Furthermore, fibers of an acceptable size and without beads were obtained in sample C. According to the morphological data reported in Table 2, the minimum fiber diameter achieved was 950 ± 390 nm. It seems that increasing the amount of PGS in the PGS-PLLA blend and decreasing feed rate are responsible for the formation of the smaller diameter fibers [16].

Cell attachment and proliferation are considerably affected by fiber diameter of the electrospun scaffold. For instance, adhesion and proliferation of endothelial cells have been observed to occur more effectively around fibers of smaller diameters than around those of cell diameter (< 5 μm). Moreover, electrospun scaffolds of small enough fiber diameters have been observed to exhibit high survival rates and good surgical and mechanical properties in the arterial graft model. This has been attributed to porosity, as one of the most important parameters in vascular grafts, that can be better controlled in the electrospinning technique [24]. These pores are of great importance as they allow vessels and endothelial cells to penetrate into the scaffold and grow, migrate, and reconstruct due to the sufficient space provided (i.e., > 5 μm for the penetration of vessel SMCs and < 5 μm for that of endothelial cells) [24, 25].

Samples (c) and (e) were selected for the subsequent tests in this study on the basis of their desirable fiber uniformity and diameter as well as their bead-free fibers.
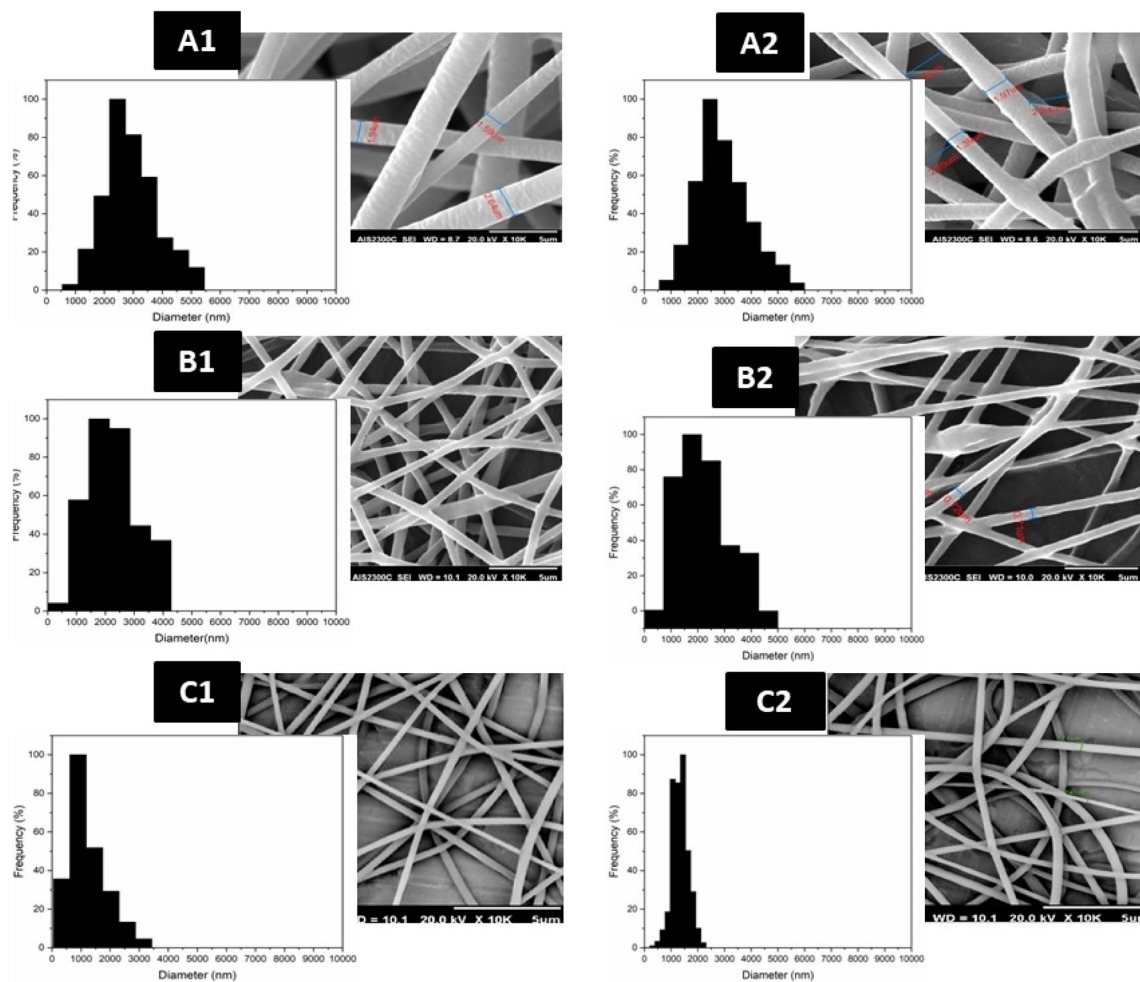
Mechanical Properties

Tensile Test

The bead free samples A2, B1, and C1 that exhibited a higher uniformity in their SEM images were selected for mechanical evaluation. Sample A2 recorded a tensile strength and an elastic modulus of 9.3 ± 0.26 MPa and 7.5 ± 0.62 MPa, respectively, due to its higher diameter and PLLA content. These values were far from those reported for coronary arteries; hence, A2 was excluded from the study.

Figure 3 depicts the mechanical behaviors of samples B1 and C1. It could be seen that the scaffolds exhibit lower stiffness values at lower tension levels (in the range of natural blood pressure). In contrast to the report by Karimi et al. [26], sample C1 at normal blood pressure exhibited a mechanical behavior similar to that of the coronary artery. One of the hemodynamic forces acting on blood vessel walls is that of tensile stress, which is the force acting on vessel wall in the circumferential direction due to its stretch. Investigating the layer-specific mechanical properties of human coronary arteries in several cases, Holzapfel et al. showed the non-linear elastic behavior (between 0 and 100 KPa) of these arteries. Claes et al. studied the mechanical behavior

Fig. 2 SEM images and the frequency histogram of the fiber size were presented in three different pre-PGS-PLLA ratios according Table 1

(stress and stretch) of coronary arteries in physiological conditions (0–240 mmHg = 0–30 KPa) through tensile tests. Their results were consistent with those reported by Holzapfel et al. Investigation of the mechanical behavior of the PGS/PLLA scaffold fabricated in the above range revealed a nonlinear elastic behavior, too. This could have been due to changing the fiber direction of the scaffold and the inherent properties of the polymers used. The stress–strain behavior, however, was similar to that of coronary arteries [27, 28].

Samples B1 and C1 recorded mean ultimate tensile strengths (UTS) of 1.6 ± 0.32 MPa and 0.420 ± 0.23 MPa, respectively, while their elastic moduli at the blood pressure range were calculated at 3.1 ± 0.35 MPa and 2.05 ± 0.27 MPa, respectively. Elastic modulus for healthy arteries is reportedly about 1.5 ± 0.55 while longitudinal and axial strengths in the LAD intima are 391 ± 144 kPa and 394 ± 223 kPa, respectively. Clearly then, elastic modulus and UTS values close to those of LAD artery intima are recorded for sample C1 as compared with sample B1 [28]. Thus, sample C1 with a pre-PGS to PLLA ratio of 3:1 offers

a superior scaffold with respect to mechanical properties and seems to be the appropriate blend for use as a scaffold in the reconstruction of intima (Table 3).

The PGS/PLLA scaffold has been synthesized via the core–shell electrospinning method, in which PGS is placed at the center and PLLA employed as a peripheral layer to yield a tensile strength of 1 ± 0.2 MPa. Such a structure has been found suitable for skin, ligament, heart muscle, and tendon applications. The scaffold has also been used to culture nerve cells with satisfactory results achieved in the nerve tissue [31]. Given the crucial role of the scaffold in the cell micro-environment, its mechanical properties and their effects on cell morphology and differentiation have received much attention among researchers. Differences in elastic modulus at the anastomosis site cause turbulence in blood circulation to hamper the endothelium and platelet activities. This, in turn, results in thrombosis, inadequate porosity, inadequate cell growth, over-proliferation of SMCs, and calcium deposition with thromboembolism [3, 4, 29, 30]. Our results
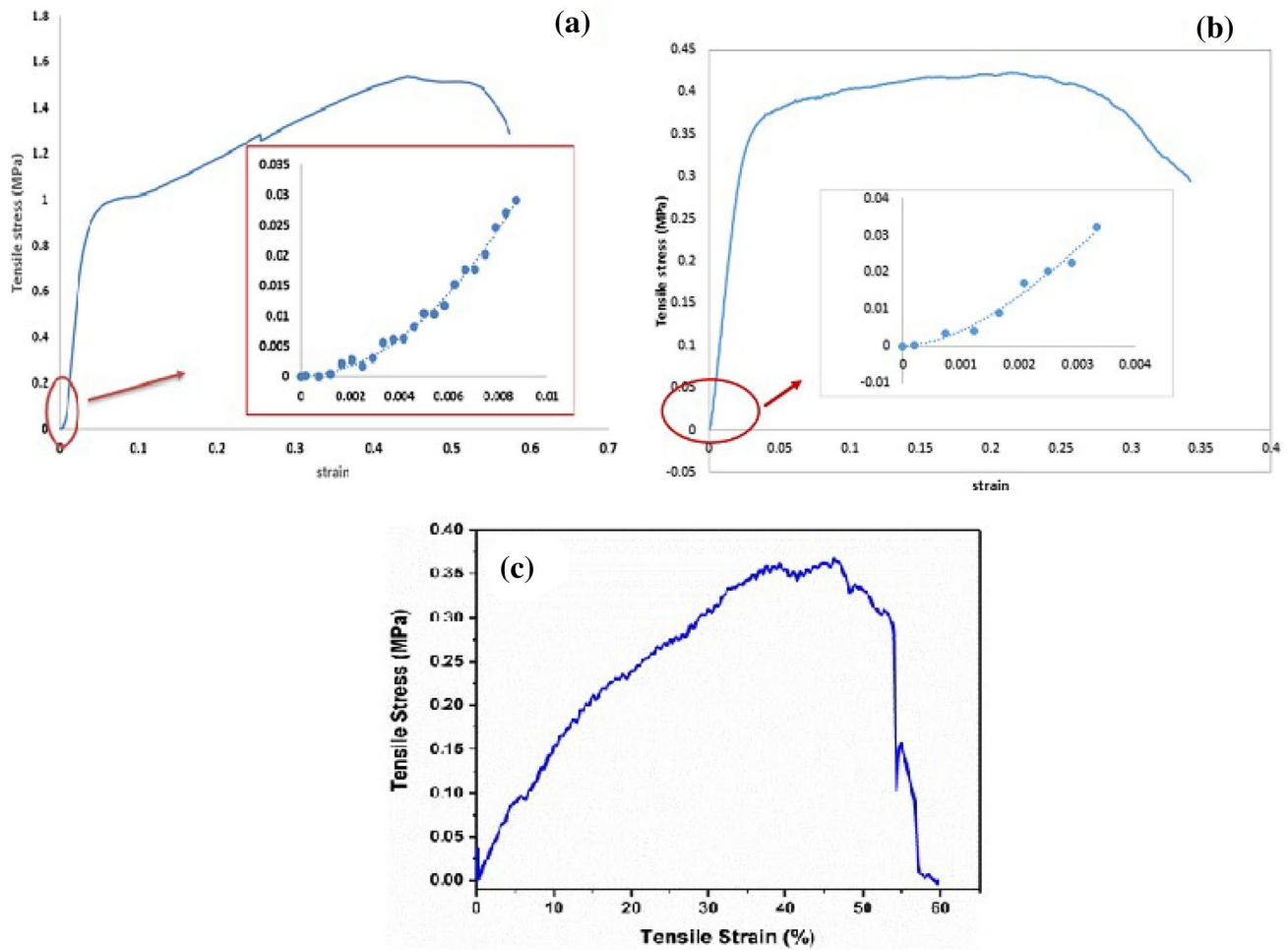
Fig. 3 Mechanical properties **a** mechanical behavior of B1 scaffold, **b** mechanical behavior of C1 scaffold, **c** pre- PGS-PLLA scaffold suture strength

Table 3 Comparison of mechanical properties of the electrospun nanofibers and LAD normal intima

Sample	B1	C1	LAD intima [28]
UTS (MPa)	1.38 ± 0.32	0.42 ± 0.23	Longitudinal: 391 ± 144 kPa Axial: 394 ± 223 kPa
Elastic modulus (MPa)	3.1 ± 0.35	2.05 ± 0.27	1.5 ± 0.55
Failure strain (%)	33 ± 7	53.17 ± 13	62 ± 2.3

show that the elastic modulus and tensile strength of the pre-PGS:PLLA (3:1) are roughly equivalent to those of biological implants used for coronary artery vessel grafts, indicating the appropriateness of this scaffold for use in vascular tissue engineering.

Based on the mechanical test and SEM results, the best sample in this study was found to be the e ones and it was, hence, used in the following steps of the study.

Burst Strength

Burst strength is an important parameter to be considered in the synthesis of vascular grafts. A burst strength of 90.2 ± 0.95 kPa (~ 675.055 mmHg) was obtained in this study for sample C1, which is consistent with that reported in Shantilal [30]. The vascular prostheses (e.g., PTFE) commonly used in surgeries and treatment of coronary

artery diseases are characterized by burst strengths of about 600 mmHg. This is while burst strengths of 5000, 1599 ± 877, and 3196 ± 1264 mmHg have been reported for internal carotid artery, native saphenous vein, and native internal mammary artery, respectively [32].

The burst strengths measured in this study were lower than those of vessels. It should, however, be noted that these layers were designed to enhance the intima characteristics and to yield an elastic modulus close to that of intima at natural blood pressure [33]. It is, therefore, essential to provision supporting layers as means to enhance the burst strength of the graft. Hence, a supporting layer is also required.

Suture Strength

The blend scaffold/ Prolene suture recorded a suture strength and failure strain of 0.360 ± 0.106 MPa and $67.6 \pm 10.97\%$, respectively (Fig. 3). Suture strength play an important role in the attachment of the scaffold to the adjust tissue. Since Prolene suture 7–0 is used in most vascular graft surgeries, it can be used to stitch the scaffold to the damaged intima or to another vascular layer. In fact, the scaffold can be resistant to Prolene or other sutures with similar failure strengths [9, 13].

Degradability

Figure 4 depicts the weight loss of the pre-PGS-PLLA (3:1) scaffold after sixty days. Clearly, the scaffold maintained its integrity but lost 60% of its total weight throughout the study period. According to Fig. 4a, the degradation process might be divided into the following three stages. In the first stage, a weight loss of about 30% occurred during ten days. Due to the high degradation rate of PGS, the fast degradation rate of the pre-PGS-PLLA (3:1) scaffold in the first stage may be attributed to part of the PGS placed on fiber surface and the interactions of its functional groups when exposed to

the PBS solution [17]. Because of the very low degradation rate of Polylactic acid, the second stage recorded a slower degradation rate since a weight loss of 30% occurred in this stage over 50 days. Apparently, polylactic acid delayed the availability of the PGS's functional groups to the PBS solution, thereby lowering the degradation rate. Degradation rate was observed to intensify in the third stage as a result of the penetration of PBS into the fibers, giving rise to the simultaneous degradation of both polylactic acid and PGS. This is because the area inside the fibers becomes locally acidic upon the penetration of PBS into the PGS fibers to accelerate PLLA destruction. This is illustrated by the increased slope of the demolition diagram in the third area.

Polyglycerol sebacate enhances the scaffold's hydrophilicity. This controls its degradation to lead to the growth and proliferation of SMCs and autologous endothelial cells and, thereby, to intima's reconstruction [4].

Contact Angle

Water droplets were scattered on the electrospun pre-PGS-PLLA (3:1) blend scaffold and allowed to soak for a few seconds. As seen in Fig. 4b, the structure was found to be highly hydrophilic so that the contact angle between water and the surface was less than 10◦.

The results revealed the dependence of contact angle on both surface type and morphology. The pre-PGS content of the sample was high and the fiber surface was mainly covered with this hydrophilic compound. Figure 5 depicts the molecular structure of the PGS pre-polymer, indicating its hydrophilic nature due to the presence of unreactive OH groups. Clearly, the high hydrophilicity of the scaffolds led to proper cell adhesion and blood compatibility [16, 33].

In contrast, the electrospun PLLA scaffold imitates the ECM in terms of structure. However, its low hydrophilicity leads to lower cell attachment and proliferation. The contact
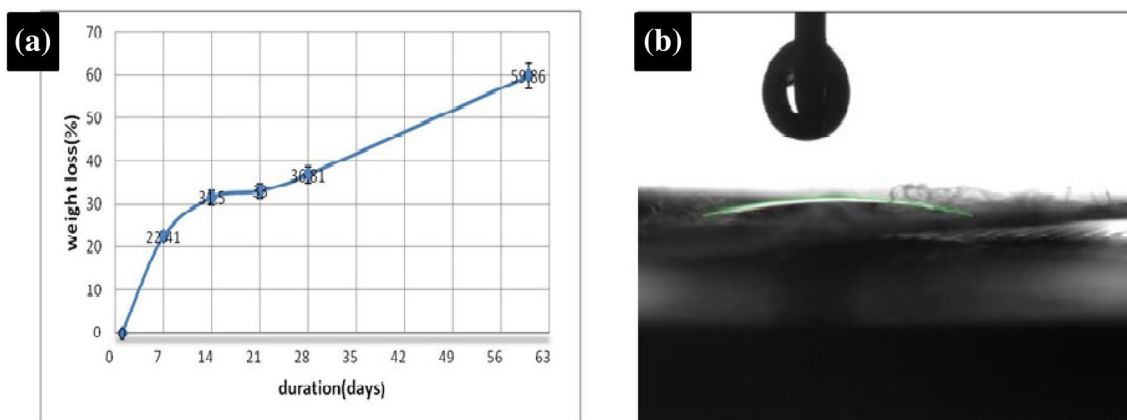
Fig. 4 **a** The weight loss of pre-PGS-PLLA (3:1) scaffold after 60 days, **b** contact angle of water with pre-PGS-PLLA (3:1) blend scaffold
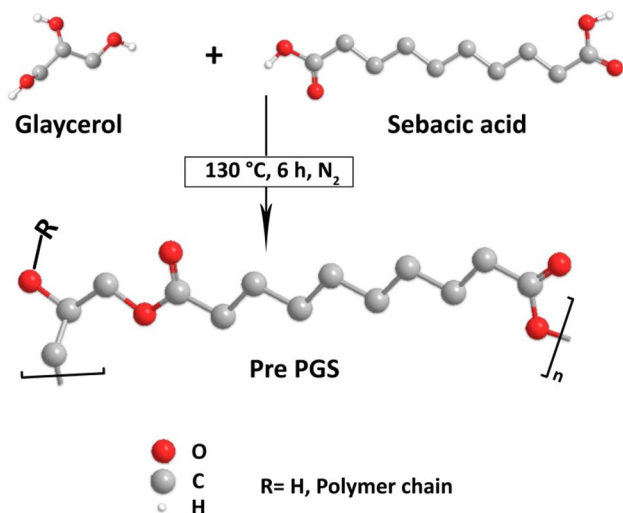
Fig. 5 Molecular structure of pre-PGS

angle of PLLA scaffolds is reportedly $125 \pm 2°$, indicating the hydrophobic nature of these scaffolds. On the other hand, pre-PGS is highly hydrophilic, and numerous studies have been carried out to add both hydrophilic and hydrophobic compounds to scaffolds in order to improve cellular behavior [16].

Cellular Tests

Cell Toxicity, Attachment and Morphology

The results of HUVEC cell culture on the pre-PGS-PLLA scaffold are presented in Fig. 6. It is seen that there is no significant difference between the control and the test samples, indicating the non-toxicity of the scaffold. The significant difference between cell growths through the first to the fifth day indicates the proper growth and proliferation of HUVEC cells on the scaffold. This might be attributed to the scaffold's good hydrophilic properties and its appropriate
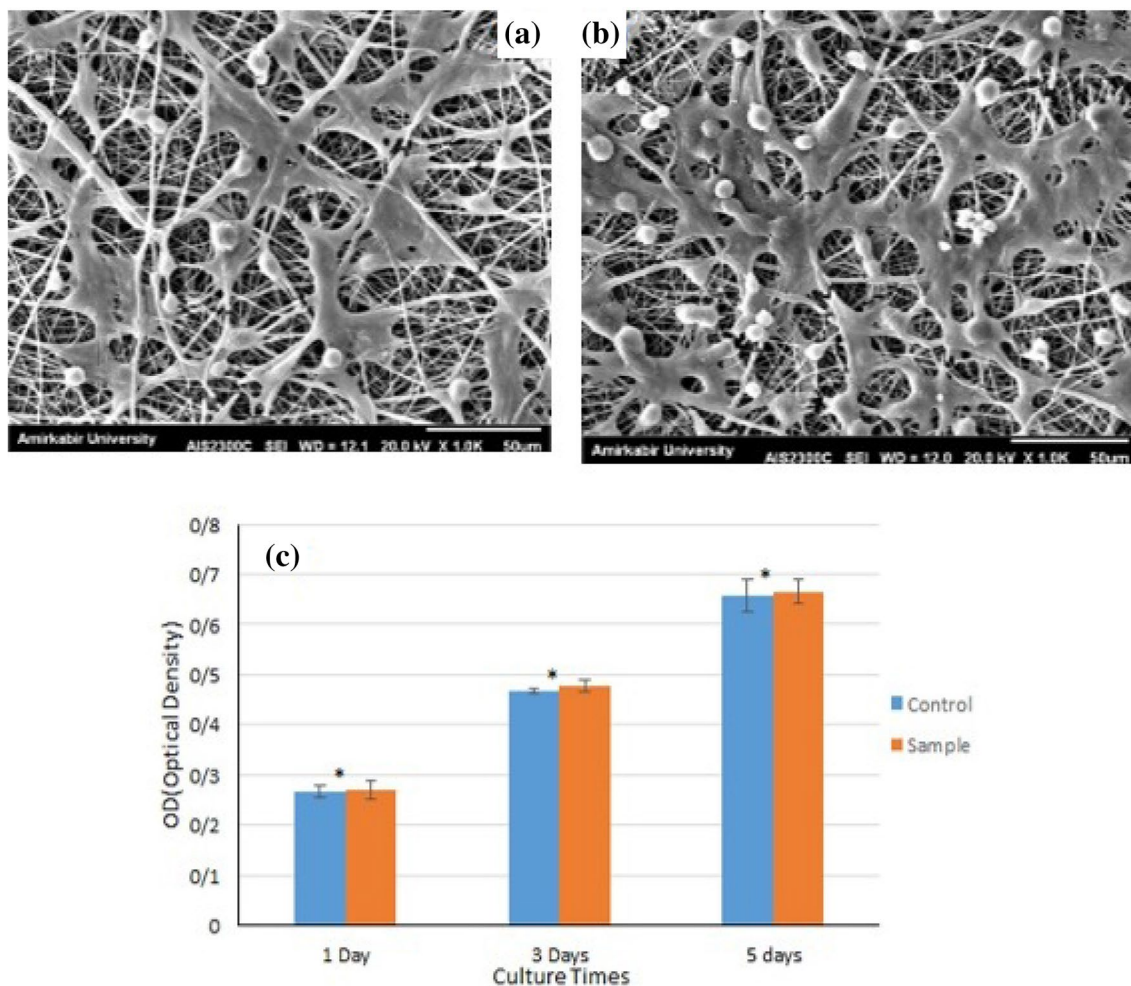

Fig. 6 The SEM micrograph of HUVEC (NCBI C554) on pre-PGS-PLLA (3:1) scaffold Cell attachment **a** after 3 days, **b** after 5 days, **c** viability and proliferation of HUVEC cells on the pre-PGS-PLLA scaffold with an optimized ratio (3:1)

elastic modulus, which led to the satisfactory adaption of endothelial cells [33]. As a result, the endothelial cells attached properly to the scaffold, entered the proliferative phase, and generated colonies favorable to the proper growth and proliferation of the cells. It may be claimed that the hydrophilic scaffold provides a more favorable environment for the attachment and growth of HUVEC cells so that the endothelial cells were able to propagate well in all directions due to the random arrangement of the fibers [7]. As seen in Fig. 6, the cells not only had cytoplasmic appendages and a normal morphology but often formed colonies and interacted with adjacent cells as well. In addition to their proper proliferation and attachment, the cells showed natural morphological conditions. When cultured on a surface, cells are capable of sensing the different physical signals such as substrate stiffness in their environment and reacting to them appropriately through receptor-ligand interactions. This process takes place through application of force and the elastic reaction of the substrate, which leads to the conversion of mechanical signals into biochemical signals in a process known as mechano-transduction. In the human body, there are hard and soft tissues with a wide range of stiffness moduli, ranging from 10 GPa for the bones to 3 kPa for the liver [34].

Thus, cells experience environments with different stiffness levels affecting their mechano-transduction. In the circulatory system, endothelial cells are exposed to varying degrees of stiffness under different physiological and pathological conditions that can directly affect their function. Endothelial function and morphology can be altered in response to changes in the inner membranes of the vessels. Moreover, surface stiffness might affect several cell behavioral parameters such as morphology, proliferation, migration, life, attachment, and differentiation [3, 35]. Attachment of cells to the substrate applies a stretch force to cause a microstrain depending on the thickness and elastic modulus of the substrate. This, in turn, can modulate cell behavior. Given the viability of cells on the substrate ($< 50\%$), thin substrates provide conditions favorable to the attachment of cells 24 h after culture. This might be due to the lamellipodia and filopodia that facilitate cell attachment on the scaffold [6, 7]. It was observed in the present study that the elastic modulus of the fabricated scaffold allowed for a significant viability rate. On the other hand, a statistically acceptable cell life was observed in the experimental groups 24, 72, and 120 h after culture. Moreover, proper thickness of the scaffold can reportedly increase cell proliferation regardless of its elastic modulus [7, 33].

Unlike the many articles (e.g., Wang et al. [19]) that focused on the effects of the substrate's elastic modulus on cell morphology, growth, and proliferation, the present study simply concentrated on fabricating scaffolds with proper mechanical properties similar to the natural conditions.

Moreover, the degradability and toxicity of the scaffold was duly investigated. The findings of the study indicate that the elastic modulus of the scaffold fabricated is consistent with that reported in Goli et al. [7] and that the cell morphology is desirable due to the good hydrophilicity of the scaffold. However, it was found that the elastic modulus of the scaffold had significant effects on cell proliferation. The interaction between cells and extremely thin substrates might lead to a cellular behavior distinct from that of cells on thick layers as thicker layers with high elastic moduli behave like thick matrices. Goli et al. [7]showed that HUVEC cells were able to make rich filopodia and lamellipodia on scaffolds with elastic moduli rarely above 2 MPa. It is, therefore, essential to vary the elastic modulus of thick layers in order to achieve the best cell behavior. Since HUVEC's behavior depends on such mechanical properties of the scaffold as thickness and elastic modulus, they exhibit differences in their morphology, viability, and growth [3, 7]. It might be argued that the mechanical environment can modulate cell signaling under different biological conditions such as atrogenesis, morphogenesis, growth, and repair in which adjacent cells receive signals from each other. Scaffold deformability provides a signal amplitude that the cells sense in vitro, although other parameters such as cell phenotype, cell number, and culture conditions also regulate these effects. In addition to the creation of favorable culture conditions, the mechanical properties of the scaffold can also affect such basic parameters of cell behavior as attachment and motility. Motility as a morphological characteristic is considered to be the main kinetic process after cell attachment when the cells are placed on the substrate, so that the cells evaluate their micromechanical environment with respect to the substrate and reconstruct themselves by attaching and applying tensile forces to the substrate. The resistance of the substrate as realized by its stiffness and deformability against the applied cellular force can modulate cell behavior. Substrate deformability varies with its elastic modulus and thickness. However, the tensile forces imposed by HUVECs can lead to significant deformations regardless of the substrate's elastic modulus [3].

As can be seen in Fig. 6, cell viability is about 100% and almost constant over time with no evidence of toxicity at the different stages of testing.

Conclusion

This study was conducted to achieve a scaffold appropriate for intima reconstruction through optimizing the parameters of the pre-PGS-PLLA blend. The results showed that the use of pre-PGS-PLLA (3:1) blend resulted in a UTS of 0.42 ± 0.23 MPa and an elastic modulus of 2.05 ± 0.27 MPa, which are close to those reported for intima. The literature

review showed that the ultimate tensile strengths of both the medium and intima are very close. Hence, the mechanical properties of the scaffolds synthesized through tissue engineering should be close to those of the original tissue to provide sufficient scaffold strength once placed and, thereby, avoid removal by blood flow. Moreover, the scaffold should be as flexible as the natural vessel is. The scaffold fabricated in this study was observed not only to maintain its integrity during degradation but exhibited good hydrophilic properties as well. Cell test results also confirmed the non-toxicity of the fabricated scaffold that allowed satisfactory cell growth and proliferation with desirable cellular morphology. These advantageous properties enable the scaffold to reconstruct properly the intima layer in terms of both mechanical properties and cellular response. Interestingly, the synthesized scaffold exhibited mechanical properties quite similar to those of the media in the artery. For future study, an outermost supporting layer may be suggested to be designed in order to ensure better burst strengths and to achieve an ideal scaffold as a synthetic vascular graft.

References

1. Lee AY, Lee Y-U, Mahler N et al (2014) Regenerative implants for cardiovascular tissue engineering. Transl Res 163(4):321–341
2. Song HG, Rumma RT, Ozaki CK et al (2018) Review vascular tissue engineering : progress, challenges, and clinical promise. Stem Cell 22:340–354
3. Goli-Malekabadi Z, et al. (2017) Effects of substrate deformability on cell behaviors: elastic modulus versus thickness. J Mech Med Biol 17(05):1750088
4. Wadey K, Lopes J et al (2018) Role of smooth muscle cells in coronary artery bypass grafting failure. Cardiovasc Res 114(4):601–610
5. Jeon H, Tsui JH, Jang SI et al (2015) Combined effects of substrate topography and stiffness on endothelial cytokine and chemokine secretion. ACS Appl Mater Interfaces 7:4525–4532
6. Knecht DA, Xue F, Janzen DM (2010) Contribution of filopodia to cell migration: a mechanical link between protrusion and contraction. Int J Cell Biol. https://doi.org/10.1155/2010/507821
7. Goli-Malekabadi Z, et al. (2017) Time dependency of morphological remodeling of endothelial cells in response to substrate stiffness. BioImpacts 7(1):41–47
8. Pashneh-Tala S, MacNeil S, Claeyssens F (2015) The tissue-engineered vascular graft—past, present, and future. Tissue Eng Part B 22(1):68–100
9. Carrabba M, Madeddu P (2018) Current strategies for the manufacture of small size tissue engineering vascular grafts. Front Bioeng Biotechnol 6:1–12
10. Putzu M (2015) Biopolymeric Scaffold obtained by Electrospinning for Intima Vessel regeneration. Biopolymeric Scaffold obtained by Electrospinning for Intima Vessel regeneration. Università degli Studi di Napoli Federico II. 104
11. Javanmard SH, JAnari J (2016) Anari J (2016) In vitro hemocompatibility and cytocompatibility of a three-layered vascular scaffold fabricated by sequential electrospinning of PCL collagen, and PLLA nanofibers. J Biomater Appl 31(3):438–449
12. Miyachi H, Takahashi M, Komori K (2015) A novel approach against vascular intimal hyperplasia through the suppression of girdin. Ann Vasc Dis 8:69–73
13. Awad NK, Niu H, Ali U (2018) Electrospun fibrous scaffolds for small-diameter blood vessels : a review. Membranes 8:1–26
14. Zhou Z, Zhao X, Coates YL et al (2017) Structure and blood compatibility of highly oriented poly(lactic acid)/thermoplastic polyurethane blends produced by solid hot stretching. Polym Adv Technol 24(9):853–860
15. Yan Y, Sencadas V, Jin T et al (2017) Tailoring the wettability and mechanical properties of electrospun poly(L-lactic acid)-poly(glycerol sebacate) core-shell membranes for biomedical applications. J Colloid Interface Sci 508:87–94
16. Frydrych M, Chen B (2013) Large three-dimensional poly(glycerol sebacate)-based scaffolds: a freeze-drying preparation approach. J Mater Chem B 1:6650
17. Salehi S, Czugala M, Stafiej P et al (2017) Acta Biomaterialia scaffold as intrinsic bio- and immunocompatible system for corneal repair. Acta Biomater 50:370–380
18. Xu B, Li Y, Zhu C et al (2015) Fabrication, mechanical properties and cytocompatibility of elastomeric nanofibrous mats of poly (glycerol sebacate). Eur Polymer J 64:79–92
19. Jia Y, Wang W et al (2016) Synthesis and characterization of poly(glycerol sebacate)-based elastomeric copolyesters for tissue engineering applications. Polym Chem 7(14):2553–2564
20. Li X, Hong AT, Naskar N, Chung H (2015) Criteria for quick and consistent synthesis of poly(glycerol sebacate) for tailored mechanical properties. Biomacromol 16(5):1525–1533
21. Semnani D, Morshed M (2007) A novel method for porosity measurement of various surface layers of nanofibers mat using image analysis for tissue engineering applications. J Appl Polym Sci 106:2536–2542
22. Meng X, Wang X (2019) Suture retention strength of P(LLA-CL) tissue-engineered vascular grafts. RSC Adv 9(37):21258–21264
23. Shi H, Gan Q, Liu X et al (2015) RSC advances regeneration. RSC Adv 5:79703–79714
24. Yalcin Enis I, Gok Sadikoglu T (2016) Design parameters for electrospun biodegradable vascular grafts. J Ind Text 47(8):2205–2227
25. Wang K, Zheng W, Pan Y et al (2016) Three-layered PCL grafts promoted vascular regeneration in a rabbit carotid artery model. Macromol Biosci 16(4):608–618
26. Karimi A, Navidbakhsh M, Shojaei A et al (2014) Study of plaque vulnerability in coronary artery using Mooney-Rivlin model: a combination of finite element and experimental method. Biomed Eng 26(01):1450013
27. Claes E, Atienza JM, Rojo FJ, et al (2010) Mechanical Properties of Human Coronary Arteries. In: 2010 Annual International Conference of the IEEE Engineering in Medicine and Biology 2010 Aug .IEEE. 3792–3795
28. Holzapfel GA, Sommer G, Gasser CT et al (2005) Determination of layer-specific mechanical properties of human coronary arteries with nonatherosclerotic intimal thickening and related constitutive modeling. Am J Physiol 289(5):H2048–H2058
29. Marsden AL, Truskey GA, Marsden AL, Truskey GA (2018) Science direct the future of biomedical engineering – vascular bioengineering. Curr Opin Biomed Eng 5:3–5
30. Shantilal D, Vara B (2009) Development of a coronary artery bypass graft with the aid of tissue engineering : Investigation of gene expression on seeded compliant 34 nanocomposite conduits

A thesis submitted for the degree of Doctor of Philosophy (Ph.D) By

31. Xu B, Rollo B, Stamp LA et al (2013) Non-linear elasticity of core/shell spun PGS/PLLA fibres and their effect on cell proliferation. Biomaterials 34:6306–6317

32. Konig G, Mcallister TN, Dusserre N et al (2009) Biomaterials Mechanical properties of completely autologous human tissue engineered blood vessels compared to human saphenous vein and mammary artert. Biomaterials 30:1542–1550

33. Hassan MI, Chong LH, Sultana N (2016) Wettability and water uptake properties of PLA and PCL/Gelatin-based electrospun scaffolds. ARPN J Eng Appl Sci. 23(11):13604–13607

34. Van Eijden TMGJ, Van Ruijven LJ, Giesen EBW (2004) Bone tissue stiffness in the mandibular condyle is dependent on the direction and density of the cancellous structure. Calcif Tissue Int 75:502–508

35. Discher DE, Janmey P, Wang Y (2005) Tissue cells feel and respond to the stiffness of their substrate. Science 310:1139–1144

Publisher's Note Springer Nature remains neutral with regard to jurisdictional claims in published maps and institutional affiliations.